

Discretization methods with analytical characteristic methods for advection-diffusion-reaction equations and 2d applications.

Jürgen Geiser

Humboldt-Universität zu Berlin
Unter den Linden 6
D-10099 Berlin, Germany
`geiser@mathematik.hu-berlin.de`

Abstract. Our studies are motivated by a desire to model long-time simulations of possible scenarios for a waste disposal. Numerical methods are developed for solving the arising systems of convection-diffusion-dispersion-reaction equations, and the received results of several discretization methods are presented. For the methods we allow large time steps to reach major simulation periods of about 10,000 [a]. For that we use higher-order discretization methods, which allow us to use large time steps without losing accuracy. By decoupling a multi-physical and multi-dimensional equation, simpler physical and one-dimensional equations are obtained and can be discretized with higher-order methods. The results of each equation are thereby coupled with an operator-splitting method. The discretization methods are described for the convection-reaction equation and for the diffusion-dispersion equation. Both are based on finite volume methods, which elements are centered in vertices. For the convection-reaction equation a new modified discretization method is presented by embedding analytical one-dimensional solutions in the multi-dimensional finite volume methods. Using meliorated higher-order operator-splitting methods, we can improve our methods for the solution of the full equations. Some applications containing this methods are computed with the underlying program tool R^3T , and the main concepts are presented. A benchmark problem based on analytical solutions is introduced for testing the new discretization method and for presenting higher-order results. Furthermore, a complex problem for the simulation of radioactive waste disposals with underlying flowing groundwater is presented. The transport and reaction simulations for the decay chains are presented in 2d realistic domains, and we discuss the received results. At the end, we present our conclusions and outlook for further works.

1 Introduction

Our studies are motivated by a desire to model the transport of radioactive and chemical contaminants through an overlying rock. We are interested, in particular, in the long-time contamination of the underlying porous media. The

mathematical model provides us with a coupled system of convection-diffusion-dispersion-reaction equations. To solve such equation systems on different scales, we have to deal with adapted discretization and solver methods. One main idea is to split the full equation system and solve each simpler equation on the adapted time scale. For such a splitting we apply and develop improved algorithms regarding our target to achieve higher efficiency and more exact accuracy. For the small scales, where the reaction equations as well as the convection equations belong to, we use the explicit temporal discretization. For the larger scales, appertaining equations are the diffusion and dispersion equations, we use the implicit temporal discretization. The spatial discretization methods deal with the finite volume methods for all spatial terms. For more accuracy we apply the characteristic method as an underlying discretization method on the convection equations on fast scales. A mixture is presented for the convection-reaction equation on the same scales, where we embed the analytical solutions of the one-dimensional convection-reaction equations, which are limited by the CFL condition. Higher-order methods are used by reconstruction with linear test functions. For the diffusion-dispersion equation we use the implicit temporal discretization and the standard finite volume methods. The underlying linear system of equations is solved iteratively with a multi-grid solver. Our main advantage in this context is the coupling of the different equation types to obtain higher-order discretization methods. The methods are verified by benchmark problems and the numerical results are compared with the analytical solutions. A real-life problem is presented as a simulation of a waste disposal with realistic parameters and underlying layers in the porous media. The calculations are presented with figures and convergence results.

The paper is outlined as follows. We introduce our mathematical model of a contaminant transport in flowing groundwater in section 2. In section 3 we introduce the finite volume methods to be used as basic discretization methods for our different equations. The modifications on the finite volume methods with respect to each equation type are explained in section 4 for the convection part, in section 5 for the reaction part, in section 6 for the mixture of convection and reaction equations, and in section 7 for the diffusion-dispersion part. The operator-splitting methods are presented in section 8. Our numerical results with benchmark problems and realistic waste disposals are described in section 9. Finally we discuss our future works in section 10 with respect to our research area.

2 Mathematical model

We consider a steady state groundwater flow, that is described by a given velocity field $\mathbf{v} = \mathbf{v}(x)$ for $x \in \Omega \subset \mathbb{R}^d$ for $d = 2$ or $d = 3$. In the groundwater several radionuclides (or some other chemical species) are dissolved.

We suppose, that these nuclides take part in irreversible, first-order chemical reactions. Particularly, each nuclide (a “mother”) can decay only to a single

component (to a “daughter”), whereby each nuclide can be produced by several reactions, i.e. each daughter can have several mothers.

Moreover, the radionuclides can be adsorbed to the soil matrix. If equilibrium linear sorption is assumed with different sorption constants for each component, the advective-dispersive transport of each component is slowed down by a different retardation factor.

Summarizing, the mathematical model can be written in the form, see [4, 5, 12],

$$R^{(i)}\phi\left(\partial_t u^{(i)} + \lambda^{(ij)}u^{(i)}\right) + \nabla \cdot \left(\mathbf{v}u^{(i)} - D^{(i)}\nabla u^{(i)}\right) = \sum_k R^{(k)}\phi\lambda^{(ki)}u^{(k)}, \quad (1)$$

where $i = 1, \dots, I_u$. The integer I_u denotes the total number of involved radionuclides. A stationary groundwater is supposed by considering only divergence-free velocity fields, i.e.

$$\nabla \cdot \mathbf{v}(x) = 0, \quad x \in \Omega. \quad (2)$$

The unknown functions $u^{(i)} = u^{(i)}(t, x)$ denote the concentrations of radionuclides, where the space and time variables (t, x) are considered as $t \geq 0$ and $x \in \Omega$. The constant reaction rate $\lambda^{(ij)} \geq 0$ determines the decay (sink) term $\lambda^{(ij)}u^{(i)}$ for the concentration $u^{(i)}$ and the production (source) term for the concentration $u^{(j)}$. In general, the j -th radionuclide needs not to be included in the system (1), i.e. $j > I_u$. The indices k in the right hand side of (1) run through all mothers of the i -th radionuclide.

The remaining parameters in (1) include the diffusion-dispersion tensors $D^{(i)} = D^{(i)}(x, \mathbf{v})$, cf. [5], the retardation factors $R^{(i)} = R^{(i)}(x) \geq 1$, and the porosity of the medium $\phi = \phi(x) > 0$.

In the following we concentrate on the modeling of processes on the boundary $\partial\Omega$ of the domain Ω and describe inflow and outflow boundaries.

We apply standard inflow and outflow boundary conditions. Particularly, we neglect the diffusive-dispersive flux at the outflow (and “noflow”) boundary $\partial^{out}\Omega := \{x \in \partial\Omega, \mathbf{n} \cdot \mathbf{v} \geq 0\}$,

$$\mathbf{n} \cdot D^{(i)}\nabla u^{(i)}(t, \gamma) = 0, \quad t > 0, \quad \gamma \in \partial\Omega, \quad (3)$$

where \mathbf{n} is the normal unit vector with respect to $\partial\Omega$. For the inflow boundary $\partial^{in}\Omega := \{x \in \partial\Omega, \mathbf{n} \cdot \mathbf{v} < 0\}$ we assume, that the concentrations are prescribed by Dirichlet boundary conditions

$$u^{(i)}(t, \gamma) = U^{(i)}(t, \gamma), \quad t > 0, \quad \gamma \in \partial^{in}\Omega, \quad (4)$$

where the functions $U^{(i)}$ describe the boundary condition in the inflow boundary, see [19].

The initial conditions are considered in a general form,

$$u^{(i)}(0, x) = U^{(i)}(0, x), \quad x \in \Omega. \quad (5)$$

Several authors present analytical solutions for the problem (1) with the assumption of an unidirectional constant velocity $\mathbf{v} \equiv (v, 0, 0)$ and special boundary and initial conditions, see [19, 34]. In this paper we introduce the finite

volume discretization method to obtain a precise numerical solution of (1) for a general form of the velocity \mathbf{v} , e.g., $\mathbf{v} = \mathbf{v}(x)$, and for the general boundary and initial conditions (3) - (5).

The basic idea of our method is to apply a new second-order, explicit discretization scheme for the advective-reactive part of the system (1). This method is based on analytical solutions for locally one-dimensional problems on boundaries between two finite volumes, analogously to the well-known Godunov algorithm for purely advective problems, cf. [28]. This numerical method is locally mass conservative and it produces numerical solutions with no unphysical oscillations.

To solve the general model (1) numerically, we have to couple this new method with some standard discretizations for the dispersion part of (1) using the operator-splitting procedure. We present a standard “vertex-centered” finite volume method (or “control-volume finite element method”, see [28]) for the discretization of the diffusive-dispersive part of the transport.

Due to the linearity of the equations in (1), we can split the problem (1) into several simpler problems. Applying afterwards the principle of superposition, we can obtain the solution of (1) by summing the solutions of such simpler problems.

These simpler systems are given for each $u^{(i)}$, where only a single linear decay chain with $u^{(i)}$ at the top is considered. As each nuclide decays only to a unique component of the system and only irreversible reactions are assumed, such decay chains are uniquely defined. Consequently, we end up with the problem of the form:

$$R^{(i)} \phi \left(\partial_t u^{(i)} + \lambda^{(i)} u^{(i)} \right) + \nabla \cdot \left(\mathbf{v} u^{(i)} - D^{(i)} \nabla u^{(i)} \right) = R^{(i-1)} \phi \lambda^{(i-1)} u^{(i-1)}, \quad (6)$$

with the Dirichlet boundary conditions at the inflow boundary for $t > 0$ and $\gamma \in \partial^{in} \Omega$

$$u^{(1)}(t, \gamma) = U(t, \gamma), \quad (7)$$

$$u^{(i)}(t, \gamma) = 0, \quad i = 2, \dots, I, \quad (8)$$

and initial conditions for $x \in \Omega$,

$$u^{(1)}(0, x) = U(0, x), \quad (9)$$

$$u^{(i)}(0, x) = 0, \quad i = 2, \dots, I. \quad (10)$$

Clearly, the non-zero boundary and initial conditions (4) - (5) are only considered for $u^{(i)}$ with all other components having zero initial concentrations and zero inflow concentrations. Moreover, for the first nuclide with concentration $u^{(1)}$ we define formally $\lambda^{(0)} = 0$, i.e. the nuclide at the top only decays. Furthermore, all reaction constants $\lambda^{(i)}$, except the last one, are supposed to be strictly positive, i.e. $\lambda^{(i)} > 0$ for $i = 1, 2, \dots, I - 1$, and $\lambda_I \geq 0$. Of course there holds $I \leq I_u$.

In fact, the problem (6) - (10) can be furthermore splitted into two simpler problems. Firstly, non-zero initial conditions (10) shall be considered with zero

concentration at the Dirichlet boundary, i.e. $U(t, \gamma) \equiv 0$ in (7), and secondly, the zero initial conditions shall be taken, i.e. $U(0, x) \equiv 0$ in (10), with general boundary conditions (7). Again, the sum of both solutions constitutes the solution of the problem (6) - (10).

Further on in this paper, we only treat the problem of the form (6) - (10).

3 Finite volume methods

The diffusion-dispersion part of the transport equation (6) will be discussed in section 7.

To solve the remaining advection-reaction part of (6) by finite volume methods, we consider a mesh of nonempty non-intersecting finite volumes $\Omega_j \subset \Omega$ that cover Ω . We assume that Ω_j , $j = 1, \dots, N$ are polygonal (consequently, Ω must be polygonal, too).

To simplify the notation, we skip the index i in (6), i.e. $u := u^{(i)}$, and we write:

$$R\phi(\partial_t u + \lambda u) + \nabla \cdot (\mathbf{v}u) = Q, \quad (11)$$

where $Q = R^{(i-1)}\phi\lambda^{(i-1)}u^{(i-1)}$.

Integrating (11) over Ω_j and some time interval (t^n, t^{n+1}) , we obtain

$$\int_{\Omega_j} R\phi u(t^{n+1}) = \int_{\Omega_j} R\phi u(t^n) - \int_{t^n}^{t^{n+1}} \int_{\partial\Omega_j} \mathbf{n}_j \cdot \mathbf{v}u + \int_{t^n}^{t^{n+1}} \int_{\Omega_j} (Q - \lambda u), \quad (12)$$

where \mathbf{n}_j is the unit normal vector with respect to the boundary $\partial\Omega_j$ of Ω_j . For simplicity, we skipped the integration variables in (12).

Furthermore, we suppose that the porosity ϕ and the retardation factor R have a piecewise constant form with respect to the finite volume mesh, i.e.

$$\phi(x) \equiv \phi_j, \quad R(x) \equiv R_j, \quad x \in \Omega_j. \quad (13)$$

For a general case of ϕ and R , we can apply some kind of averaging. Note that $R_j \geq 1$.

Finally, we denote the averaged concentration u_j^n of u at $t = t^n$ in Ω_j , i.e.

$$u_j^n := \frac{1}{|\Omega_j|} \int_{\Omega_j} u(t^n, x) dx, \quad (14)$$

where $|\Omega_j|$ denotes the volume of Ω_j . Analogously to (14), we can define the averaged values u_j^{n+1} .

Using the assumptions and notations from above, we can rewrite (12) in a discrete form,

$$|\Omega_j|R_j\phi_j u_j^{n+1} = |\Omega_j|R_j\phi_j u_j^n - \sum_k \int_{t^n}^{t^{n+1}} \int_{\Gamma_{jk}} \mathbf{n}_j \cdot \mathbf{v}u + \int_{t^n}^{t^{n+1}} \int_{\Omega_j} (Q - \lambda u), \quad (15)$$

where the index k is considered only for neighbors Ω_k of Ω_j with common surfaces, i.e. $\Gamma_{jk} := \partial\Omega_j \cap \partial\Omega_k$. Note that the subscripts j and k here are related to the finite volume mesh, and that they should not be mistaken with superscripts in (1) reserved for indices of radionuclide components.

In fact, no numerical approximation was used in (15). Before applying some second-order numerical discretization for (15) with no time-splitting discretization error, we first discuss the solutions of the purely advective and purely reactive case of our model.

4 Numerical solution of the advection equation

If no reactions are considered in (11), the remaining advection equation takes the following form:

$$R\phi\partial_t u + \nabla \cdot (\mathbf{v}u) = 0. \quad (16)$$

The initial conditions are given by (10), and $u(t, \gamma)$ is explicitly given for $t > 0$ at the inflow boundary $\gamma \in \partial^{in}\Omega$ by (7).

The exact solution of (16) can directly be defined using the so-called *forward tracking* form of characteristic curves. If the solution of (16) is known at some time point $t_0 \geq 0$ and some point $y \in \Omega \cup \partial^{in}\Omega$, then u remains constant for $t \geq t_0$ along the characteristic curve $X = X(t)$, i.e. $u(t, X(t)) = u(t_0, y)$ and

$$X(t) = X(t; t_0, y) = y + \int_{t_0}^t \frac{\mathbf{v}(X(s))}{R(X(s))\phi(X(s))} ds. \quad (17)$$

The characteristic curve $X(t)$ starts at the time $t = t_0$ in the point y , i.e. $X(t_0; t_0, y) = y$, and it is tracked forward in time for $t > t_0$. Of course, we can obtain, that $X(t) \notin \Omega$, i.e. the characteristic curve can leave the domain Ω through $\partial^{out}\Omega$.

Consequently, we have that $u(t, X(t; t_0, y)) = U(t_0, y)$, where the function $U(0, y)$ is given for $t_0 = 0$ and $y \in \Omega$ by initial conditions (10) and for $t_0 > 0$ and $y \in \partial^{in}\Omega$ by the inflow boundary conditions (7).

The solution $u(t, x)$ of (16) can also be expressed in a “backward tracking” form, that is more suitable for a direct formulation of the discretization schemes. Concretely, for any characteristic curve $X = X(t) = X(t; s, Y)$, that is defined in a forward manner, i.e. $X(s; s, Y) = Y$ and $t \geq s$, we obtain the curve $Y = Y(s) = Y(s; t, x)$, that is defined in a backward manner, i.e. $Y(t; t, X) = X$ and $s \leq t$. If we express Y as function of t_0 for $t_0 \leq t$, we obtain from (17):

$$Y(t_0) = Y(t_0; t, x) = x - \int_{t_0}^t \frac{\mathbf{v}(X(s))}{R(X(s))\phi(X(s))} ds, \quad (18)$$

and we have $u(t, x) = u(t_0, Y(t_0))$.

To simplify out treatment of inflow boundary conditions, we suppose that $U(t, \gamma) = U^{n+1/2} \equiv \text{const}$ for $\gamma \in \partial^{in}\Omega$ and $t \in [t^n, t^{n+1})$. Moreover, we define

formally for any $\gamma \in \partial^{in}\Omega$ and $t_0 \in [t^n, t^{n+1}]$, that $Y(s; t_0, \gamma) \equiv Y(t_0; t_0, \gamma)$ for $t^n \leq s \leq t_0$.

In [13], the so-called *flux-based (modified) method of characteristics* was described. This method can be deemed as an extension of the standard finite volume methods (FVMs). Using (15), the standard FVM for differential equations (16) takes the form:

$$|\Omega_j| R_j \phi_j u_j^{n+1} = |\Omega_j| R_j \phi_j u_j^n - \sum_k \int_{t^n}^{t^{n+1}} \int_{\Gamma_{jk}} \mathbf{n}_j(\gamma) \cdot \mathbf{v}(\gamma) u(t, \gamma) d\gamma dt, \quad (19)$$

The idea of a flux-based method of characteristics is to apply the substitution $u(t, \gamma) = u(t^n, Y(t^n; t, \gamma))$ on (19).

Particularly, for the integration variable $t \in (t^n, t^{n+1})$ and for each point $\gamma \in \partial^{out}\Omega_j$, the characteristic curves $Y(s)$ are tracked backward, starting in γ at $s = t$ and ending in $s = t^n$. We must reach a point $Y = Y(t^n)$, such that $Y \in \partial^{in}\Omega$ or $Y \in \Omega$. In the first case, $u(t^n, Y)$ is given by the inflow concentration $U(t^n, Y) = U^n$, in the latter one by $u(t^n, Y)$.

The integral in the right hand side of (19) can be solved exactly for the one-dimensional case with general initial and boundary conditions, see [30]. For the general 2D or 3D case, a numerical approximation of $u(t_0, Y(t_0))$, respectively of $Y(t_0)$, shall be used. Firstly, we describe such an approximation in the one-dimensional case, and afterwards for the general 2D or 3D case.

4.1 1D case with a piecewise linear form of $u(t^n, x)$.

In the one-dimensional case the domain $\Omega \subset R$ is given by an interval $(0, L)$. Due to (2) we obtain, that $v(x) \equiv v = const$ and (16) takes the form:

$$R\phi \partial_t u(t, x) + v \partial_x u(t, x) = 0, \quad x \in (0, L), \quad t \geq 0. \quad (20)$$

Next, we treat the case $v > 0$. An analogous treatment for a negative constant value of v can be easily derived.

Let the finite volume mesh consist of $J + 1$ intervals $\Omega_j := (x_{j-1/2}, x_{j+1/2})$ for $j = 0, 1, \dots, J$, where we define $x_{-1/2} \equiv x_0 = 0$ and $x_{J+1/2} \equiv x_J = L$. The length of each interval is $h_j = x_{j+1/2} - x_{j-1/2}$, and the middle points x_j for $j = 1, 2, \dots, J - 1$ are defined by $x_j := x_{j-1/2} + h_j/2$. For some illustration of the notation see figure 1.

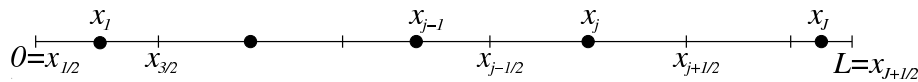


Fig. 1. Notations for the one-dimensional case of the finite volume mesh.

Let us now consider a particular form of the function u at $t = t^n$:

$$u(t^n, x) = u_j^n + \sigma_j^n(x - x_j), \quad x \in (x_{j-1/2}, x_{j+1/2}]. \quad (21)$$

This means, that $u(t^n, x)$ is a piecewise linear function with respect to the finite volume mesh with some piecewise constant slopes (gradients) σ_j^n . For a general form of u at $t = t^n$, we have to construct the function $u(t^n, x)$ of the form (21). For that, the values u_j^n can be obtained with the averaging procedure (14), the choices for the slopes σ_j^n will be discussed in the next subsection.

Using (21), we can denote the value $u(t^n, x_{j+1/2})$ at the outflow boundary point $x_{j+1/2}$ of Ω_j by

$$u_{j+1/2}^n := u_j^n + \sigma_j^n \frac{h_j}{2}. \quad (22)$$

Note that $u(t^n, x)$ for $x \in (0, L)$ is generally discontinuous over the points $x_{j+1/2}$, see figure 2 for an illustration.

The integral equation (19) can now be written in the one-dimensional form:

$$h_j R_j \phi_j u_j^{n+1} = h_j R_j \phi_j u_j^n + v \int_{t^n}^{t^{n+1}} (u(t, x_{j-1/2}) - u(t, x_{j+1/2})) dt. \quad (23)$$

We can easily show, that for $v > 0$ and some small time interval $t \in (t^n, t^{n+1})$, we have

$$u(t, x_{j+1/2}) = u(t^n, Y(t^n; t, x_{j+1/2})) \quad (24)$$

$$= u_{j+1/2}^n + (u_j^n - u_{j+1/2}^n) \frac{2v}{R_j \phi_j h_j} (t - t^n), \quad (25)$$

and we have an analogous equation for $u(t, x_{j-1/2}) = u(t, x_{(j-1)+1/2})$.

Clearly, the dependence on time of u in (24) is linear and the integral in (23) can be computed exactly using the middle point quadrature rule. For that, we denote $u_{j+1/2}^{n+1/2} := u(t^{n+1/2}, x_{j+1/2})$ and obtain

$$u_{j+1/2}^{n+1/2} = u_{j+1/2}^n + \frac{\tau^n}{\tau_j} (u_j^n - u_{j+1/2}^n), \quad (26)$$

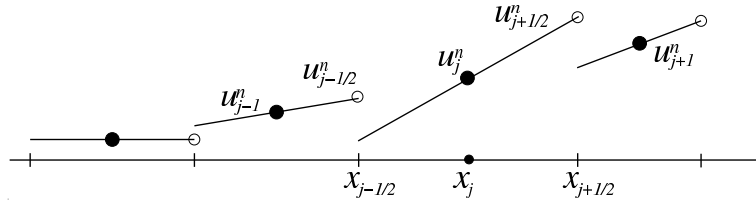


Fig. 2. Piecewise linear form of $u(t^n, x)$.

where τ_j is the so-called *critical time step*, see [13]:

$$\tau_j := \frac{h_j R_j \phi_j}{v}. \quad (27)$$

Note that $\frac{\tau^n}{\tau_j}$ in (26) represents the so-called *local grid Courant number*.

The definitions (24) - (26) are valid, only if the time step τ^n satisfies the so-called *CFL (Courant-Friedrichs-Lewy) condition* (see [28])

$$\tau^n \leq \tau_{\text{CFL}} := \min\{\tau_j, j = 0, 1, \dots, J\}. \quad (28)$$

The integral equation (23) now can be evaluated exactly for $j = 0, 1, \dots, J$ by

$$h_j R_j \phi_j u_j^{n+1} = h_j R_j \phi_j u_j^n + v \tau^n \left(u_{j-1/2}^{n+1/2} - u_{j+1/2}^{n+1/2} \right), \quad (29)$$

where $u_{-1/2}^{n+1/2} \equiv U^{n+1/2}$.

4.2 Construction of the piecewise linear form of $u(t^n, x)$.

To finalize the discretization scheme (29), we have to choose (or construct) the slopes σ_j^n . It is well-known, see [28], that σ_j^n must be chosen carefully, otherwise non-physical oscillations can be observed in the numerical solution of (29). These can include under- and overshootings of physically acceptable values for the solution.

To formulate precisely these difficulties and their solutions, we introduce the concept of flux limiters (or slope limiters) based on the local discrete minimum and maximum principle for numerical solutions of (29), as introduced in [13].

The simplest choice for the slopes σ_j^n in (21) is to set them all equal zero, so that we obtain $u_{j+1/2}^n \equiv u_j^n$. Consequently, the discretization scheme (29) turns into the well-known first-order upwind scheme

$$h_j R_j \phi_j u_j^{n+1} = h_j R_j \phi_j u_j^n + v \tau^n \left(u_{j-1}^n - u_j^n \right). \quad (30)$$

For the equations (30), the local discrete minimum and maximum principle is satisfied for $j = 1, \dots, J$,

$$\min\{u_j^n, u_{j-1}^n\} =: u_{j,\min}^n \leq u_j^{n+1} \leq u_{j,\max}^n := \max\{u_j^n, u_{j-1}^n\}, \quad (31)$$

if the CFL condition (28) is valid.

The property (31) is a consequence of the circumstance, that for (30) the trivial solution $u_j^{n+1} = u_j^n = u_{j-1}^n = 1$ is valid, that the coefficient before u_j^{n+1} in (30) is positive, i.e. $h_j R_j \phi_j > 0$, the coefficients before u_j^n and u_{j-1}^n are non-negative, i.e. $h_j R_j \phi_j - v \tau^n \geq 0$, and $v \tau^n > 0$.

To propose a higher-resolution form of (29), we can follow the approach of [28] to reconstruct the piecewise linear form of $u(t^n, x)$ in (21) by defining the slopes σ_j^n with using the values u_{j-1}^n , u_j^n and u_{j+1}^n .

Here we mention only two particular choices of σ_j^n , for other forms and more detailed discussion, see [28]. Firstly, as σ_j^n is used to define the value $u_{j+1/2}^n$ in (26), we can naturally construct the slope σ_j^n with only two values u_j^n and u_{j+1}^n ,

$$\sigma_j := \frac{u_{j+1} - u_j}{x_{j+1} - x_j}, \quad (32)$$

or, to consider all three values u_{j-1}^n , u_j^n and u_{j+1}^n , we can use the averaged gradient over (x_{j-1}, x_{j+1}) ,

$$\sigma_j := \frac{u_{j+1} - u_{j-1}}{x_{j+1} - x_{j-1}} = \frac{x_{j+1} - x_j}{x_{j+1} - x_{j-1}} \frac{u_{j+1} - u_j}{x_{j+1} - x_j} + \frac{x_j - x_{j-1}}{x_{j+1} - x_{j-1}} \frac{u_j - u_{j-1}}{x_j - x_{j-1}}. \quad (33)$$

The choice (32) leads to the so-called *Lax-Wendroff method* with

$$u_{j+1/2}^n = \frac{1}{2}(u_j^n + u_{j+1}^n), \quad (34)$$

the choice (33) leads to the so-called *Fromm method*, see [28]. A generalization of these two methods for the 2D and 3D case using unstructured grids will be presented in the next subsection.

We now formulate the conditions, that lead to the local discrete minimum and maximum principle for (29) with (32) or (33).

After substitution of (26) into (29), we obtain

$$\begin{aligned} h_j R_j \phi_j u_j^{n+1} &= \left(h_j R_j \phi_j - v \tau^n \frac{\tau^n}{\tau_j} \right) u_j^n \\ &\quad - v \tau^n \left(1 - \frac{\tau^n}{\tau_j} \right) u_{j+1/2}^n + v \tau^n u_{j-1/2}^{n+1/2}. \end{aligned} \quad (35)$$

The coefficient before $u_{j+1/2}^n$ in (35) is negative, and the discrete min-max principle (31) can not be directly obtained. Nevertheless, we can rewrite (35) into a form, where all coefficients are non-negative by introducing the values $u_{1/2+j}^n$ (using a rather formal notation):

$$u_{1/2+j}^n := 2u_j^n - u_{j+1/2}^n \quad \Rightarrow \quad u_{j+1/2}^n = 2u_j^n - u_{1/2+j}^n. \quad (36)$$

By substituting (26) and (36) to (29), we obtain

$$\begin{aligned} h_j R_j \phi_j u_j^{n+1} &= \left(h_j R_j \phi_j - v \tau^n \left(2 - \frac{\tau^n}{\tau_j} \right) \right) u_j^n + \\ &\quad + v \tau^n \left(1 - \frac{\tau^n}{\tau_j} \right) u_{1/2+j}^n + v \tau^n u_{j-1/2}^{n+1/2}. \end{aligned} \quad (37)$$

Now, we can easily show, that all coefficients in (37) are non-negative, if the CFL condition (28) is satisfied, because of

$$h_j R_j \phi_j - v \tau^n \left(2 - \frac{\tau^n}{\tau_j} \right) = v (\tau_j - \tau^n) \left(1 - \frac{\tau^n}{\tau_j} \right). \quad (38)$$

Consequently, the local discrete min-max principle can be formulated with respect to the values of u on the right hand side of (37). Of course, we want to obtain the local discrete min-max principle with respect to the values $u_{j,\min}^n$ and $u_{j,\max}^n$ defined in (31). For that the two following conditions must be fulfilled:

$$u_{j,\min}^n \leq u_{1/2+j}^n \leq u_{j,\max}^n, \quad (39)$$

$$u_{j,\min}^n \leq u_{j-1/2}^{n+1/2} \leq u_{j,\max}^n. \quad (40)$$

In general the conditions (39) - (40) are not fulfilled and we have to apply the so-called *limiters* to avoid non-physical oscillations in the numerical solution of (29), as well as the so-called *phase error*, [28].

Using the discrete min-max principle and the equivalent formulation (37) to (29), it is very easy and straightforward to formulate such limiters. The idea is to replace the value $u_{1/2+j}^n$ in (37) in the case of $u_{1/2+j}^n \notin [u_{j,\min}^n, u_{j,\max}^n]$ by the corresponding extreme value that was violated ($u_{j-1/2}^{n+1/2}$ can be replaced analogously).

Particularly, the discretization scheme (29) can be replaced by a flux-limited version

$$h_j R_j u_j^{n+1} = h_j R_j u_j^n + v \tau^n \left(\tilde{u}_{j-1/2}^{n+1/2} - \tilde{u}_{j+1/2}^{n+1/2} \right), \quad (41)$$

where

$$\tilde{u}_{j+1/2}^{n+1/2} := \begin{cases} u_{j+1,\max}^n & \bar{u}_{j+1/2}^{n+1/2} > u_{j+1,\max}^n \\ \bar{u}_{j+1/2}^{n+1/2} & u_{j+1,\min}^n \leq \bar{u}_{j+1/2}^{n+1/2} \leq u_{j+1,\max}^n \\ u_{j+1,\min}^n & u_{j+1,\min}^n > \bar{u}_{j+1/2}^{n+1/2} \end{cases}, \quad (42)$$

and

$$\bar{u}_{j+1/2}^{n+1/2} = \bar{u}_{j+1/2}^n + \frac{\tau^n}{\tau_i} (u_j^n - \bar{u}_{j+1/2}^n), \quad (43)$$

with

$$\bar{u}_{j+1/2}^n := \begin{cases} 2u_j^n - u_{j,\max}^n & 2u_j^n - u_{j+1/2}^{n+1/2} > u_{j,\max}^n \\ u_{j+1/2}^n & u_{j,\min}^n \leq 2u_j^n - u_{j+1/2}^{n+1/2} \leq u_{j,\max}^n \\ 2u_j^n - u_{j,\min}^n & u_{j,\min}^n > 2u_j^n - u_{j+1/2}^{n+1/2} \end{cases}. \quad (44)$$

The last limiter (44) is necessary to fulfill (39) for the j -th discrete equation (29).

The first limiter (42) is necessary to fulfill (40) for the $(j+1)$ -st discrete equation (29). It needs not to be used for the Lax-Wendroff discretization scheme (32), where we can directly use $\tilde{u}_{j+1/2}^{n+1/2} \equiv \bar{u}_{j+1/2}^{n+1/2}$.

The limiting procedure (42) - (44) can not fail, because the most limiting choice $\tilde{u}_{j+1/2}^{n+1/2} = u_j^n$, i.e. $\tilde{\sigma}_j^n = 0$, is always available.

The advantage of the high-resolution finite volume scheme (41) is, that it can be straightforwardly applied to 2D/3D advection equations computed on unstructured grids, see the next section.

4.3 2D/3D case

It is rather straightforward to extend the discretization scheme (41) for a 2D/3D case of the advection equation (16). To do this, we first denote

$$v_{jk} := \int_{\Gamma_{jk}} \mathbf{n}_j(\gamma) \cdot \mathbf{v}(\gamma) d\gamma. \quad (45)$$

Of course, $v_{kj} = -v_{jk}$. Further, we call a boundary Γ_{jk} of $\partial\Omega_j$ to be the “out-flow” boundary, if $v_{jk} > 0$, and, analogously, “inflow” boundary, if $v_{jk} \leq 0$. Similarly, we denote $k \in \text{out}(j)$, if $v_{jk} > 0$, and, consequently, $j \in \text{in}(k)$.

Due to $\nabla \cdot \mathbf{v}$, we have

$$\sum_{k \in \text{in}(j)} v_{kj} = \sum_{k \in \text{out}(j)} v_{jk}. \quad (46)$$

We can regard (46) as the mass conservation property for the groundwater flow in a discrete form.

In fact, a numerical approximation of v_{jk} in (45) can be used by choosing the middle point γ_{jk} of Γ_{jk} and

$$v_{jk} := |\Gamma_{jk}| \mathbf{n}_j(\gamma_{jk}) \cdot \mathbf{v}(\gamma_{jk}), \quad (47)$$

where $|\Gamma_{jk}|$ denotes the measure of Γ_{jk} . Consequently, the discrete form (46) of the mass balance property does not need to be exactly fulfilled in such a case, but very often the groundwater velocity field is given as a result of the numerical modeling, where the discrete equations (46) were included, and hence we suppose in all our next considerations, that (46) is valid.

Using the notations and approximations from above, we can approximate (19) by

$$|\Omega_j| R_j \phi_j u_j^{n+1} = |\Omega_j| R_j \phi_j u_j^n - \sum_k v_{jk} \int_{t^n}^{t^{n+1}} u(t^n, Y(t^n; t, \gamma_{jk})) dt. \quad (48)$$

The simplest discretization scheme for (48) is to assume a piecewise constant form of $u(t^n, x)$ with respect to the finite volume mesh, that means $u(t^n, x) = u_j^n$ for $x \in \Omega_j$. Consequently, for “enough small” time steps τ^n , the characteristic curves $Y(t^n; t, \gamma_{jk})$, that start at outflow boundaries $\gamma_{jk} \in \Gamma_{jk}$, remain for $t \in (t^n, t^n + \tau^n)$ in Ω_j and thus $u(t^n, Y(t^n; t, \gamma_{jk})) \equiv u_j^n$.

Using the assumptions from above, we can evaluate (48) by

$$|\Omega_j| R_j \phi_j u_j^{n+1} = |\Omega_j| R_j \phi_j u_j^n - \tau^n u_j^n \sum_{k \in \text{out}(j)} v_{jk} + \tau^n \sum_{k \in \text{in}(j)} v_{kj} u_k^n. \quad (49)$$

The discretization scheme (49) can be regarded as the first-order upwind (upstreaming) scheme. If the time step is restricted by the CFL condition $\tau^n \leq$

τ_{CFL} , see (28), then the numerical solution of (49) satisfies the local discrete minimum and maximum principle

$$u_{j,\min}^n \leq u_i^{n+1} \leq u_{j,\max}^n, \quad (50)$$

where the extreme values are given by

$$u_{j,\min}^n := \min\{u_j^n; u_k^n, k \in in(j)\}, \quad u_{j,\max}^n := \max\{u_j^n; u_k^n, k \in in(j)\}.$$

The critical time steps τ_i in (28) are now defined by

$$\tau_i := \frac{|\Omega_j| R_j \phi_j}{v_j}, \quad (51)$$

where v_j denotes the total outflow (or inflow) flux for Ω_j , i.e.

$$v_j := \sum_{k \in out(j)} v_{jk}. \quad (52)$$

The extension of the one-dimensional high-resolution scheme (29) on the 2D or 3D case can be derived in several different ways obtaining at the end several different discretization schemes. Here we present the simplest and the most straightforward one,

$$\begin{aligned} |\Omega_j| R_j \phi_j u_j^{n+1} &= |\Omega_j| R_j \phi_j u_j^n - \tau^n \sum_{k \in out(j)} v_{jk} u_{jk}^{n+1/2} \\ &+ \tau^n \sum_{k \in in(j)} v_{kj} u_{kj}^{n+1/2}, \end{aligned} \quad (53)$$

where

$$u_{jk}^{n+1/2} := u_{jk}^n + \frac{\tau^n}{\tau_i} (u_j^n - u_{jk}^n). \quad (54)$$

The value u_{jk}^n should represent (approximate) the value of u at $x_{ij} := 0.5(x_i + x_j)$. The simplest choice

$$u_{jk}^n := \frac{1}{2}(u_j^n + u_k^n) \quad (55)$$

can be regarded as the generalization of the Lax-Wendroff scheme (34). A general choice can be derived from

$$u_{jk}^n := u_j^n + \sigma_{jk}^n \cdot (x_{jk} - x_j), \quad (56)$$

where σ_{jk}^n is some reconstructed gradient used for the determination of u_{jk}^n . Later we describe a particular algorithm for the reconstruction of $\sigma_{jk}^n \equiv \sigma_j^n$ for the so-called *vertex-centered finite volumes*.

Theorem 1. *We have a second-order method for the equation (56), and our approximation error is given as:*

$$|u(t^n, x_{jk}) - u_{jk}^n| \leq O((\Delta x_{jk})^2), \quad (57)$$

where $u(x_{jk}, t^n)$ is the approximated solution and u_{jk}^n is the exact solution. Further $\Delta x_{jk} = (x_{jk} - x_j)$ is the spatial step size of the underlying grid.

Proof. Based on the literature for conservation laws, see [27, 28], we start with the reconstruction of the approximate solution u_{jk}^n given as

$$u_{jk}^n := u_j^n + \sigma_{jk}^n \cdot (x_{jk} - x_j), \quad (58)$$

where σ_{jk}^n is some reconstructed gradient used for the determination of u_{jk}^n . If we reset σ_{jk}^n with some reconstructed gradient ∇u_{jk}^n , we obtain

$$u_{jk}^n := u_j^n + \nabla u_{jk}^n \cdot (x_{jk} - x_j), \quad (59)$$

where ∇u_{jk}^n is reconstructed with the neighborhood elements, see [29, 32].

Furthermore, our analytical solution $u(x_{jk}, t^n)$ is given as:

$$u(t^n, x_{jk}) := u_j^n + \nabla u_{jk}^n \cdot (x_{jk} - x_j) + \Delta u_{jk}^n \cdot (x_{jk} - x_j)^2 + O((x_{jk} - x_j)^3). \quad (60)$$

By subtracting the analytical solution (60) of the approximate solution (59), we obtain the following error,

$$|u(t^n, x_{jk}) - u_{jk}^n| \leq O((x_{jk} - x_j)^2), \quad (61)$$

where we obtain a second-order accurate method, see also [28, 35]. This proves our statement of the theorem.

For methods higher than second order we have to approximate the second derivative of the Taylor expansion, see also [32]. It might be more delicate because of further reconstructions and limiting processes with the neighbor and neighbor-neighbor elements.

In the next step we prove the discrete min-max principle for (53). We rewrite it formally into the form

$$|\Omega_j| R_j \phi u_j^{n+1} = \left(|\Omega_j| R_j \phi_j - \tau^n v_j \left(2 - \frac{\tau^n}{\tau_i}\right) \right) u_j^n + \quad (62)$$

$$+ \tau^n \sum_{k \in \text{out}(j)} v_{jk} \left(1 - \frac{\tau^n}{\tau_i}\right) u_{jk'}^n + \tau^n \sum_{k \in \text{in}(j)} v_{kj} u_{kj}^{n+1/2}, \quad (63)$$

where the value $u_{jk'}^n$ is given analogously to (36) by

$$u_{jk'}^n = 2u_j^n - u_{jk}^n. \quad (64)$$

Based on (62), we formulate the final discretization scheme with the limiter

$$|\Omega_j| R_j u_j^{n+1} = |\Omega_j| R_j u_j^n - \tau^n \sum_{k \in \text{out}(j)} v_{jk} \tilde{u}_{jk}^{n+1/2} + \tau^n \sum_{k \in \text{in}(j)} v_{kj} \tilde{u}_{kj}^{n+1/2}, \quad (65)$$

where

$$\tilde{u}_{jk}^{n+1/2} := \begin{cases} u_{k,\max}^n & \bar{u}_{jk}^{n+1/2} > u_{k,\max}^n \\ \bar{u}_{jk}^{n+1/2} & u_{k,\min}^n \leq \bar{u}_{jk}^{n+1/2} \leq u_{k,\max}^n, \\ u_{k,\min}^n & u_{k,\min}^n > \bar{u}_{jk}^{n+1/2} \end{cases}, \quad (66)$$

and

$$\bar{u}_{jk}^{n+1/2} := \bar{u}_{jk}^n + \frac{\tau^n}{T_i}(u_j^n - \bar{u}_{jk}^n), \quad (67)$$

where

$$\bar{u}_{jk}^n := \begin{cases} 2u_j^n - u_{j,\max}^n & 2u_j^n - u_{jk}^n > u_{j,\max}^n \\ u_{jk}^n & u_{j,\min}^n \leq 2u_j^n - u_{jk}^n \leq u_{j,\max}^n \\ 2u_j^n - u_{j,\min}^n & u_{j,\min}^n > 2u_j^n - u_{jk}^n \end{cases}. \quad (68)$$

Using this approach, the so-called *grid effect* can corrupt the obtained numerical solutions and we have satisfied the discrete min-max principle. At least the result of the improved approximation is based on the middle-point rule, which preserves the min-max principle.

The next section describes the analytical solutions of the reaction-equation system.

5 Solution of the reaction-equation system

If we consider only the reaction part of the general equation (6), we have a system of ordinary differential equations,

$$\begin{aligned} R^{(1)}\phi \left(\partial_t u^{(1)} + \lambda^{(1)}u^{(1)} \right) &= 0, \quad u^{(1)}(x) = U(0, x), \\ R^{(i)}\phi \left(\partial_t u^{(i)} + \lambda^{(i)}u^{(i)} \right) &= R^{(i-1)}\phi \lambda^{(i-1)}u^{(i-1)}, \quad u^{(i)}(x) = 0, \end{aligned} \quad (69)$$

for $i = 2, \dots, I$, where the dependence on the space variable $x \in \Omega$ is realized only through initial conditions for the first component and through retardation factors $R^{(i)}$.

If all reaction constants $\lambda^{(i)}$ are different, the exact solution is given by

$$u^{(i)}(t, x) = U(0, x) \frac{R^{(1)}(x)}{R^{(i)}(x)} A_i \sum_{j=1}^i A_{j,i} \exp(-\lambda^{(j)}t), \quad (70)$$

where the constants A_i and $A_{j,i}$ for $j = 1, \dots, i$ are defined as:

$$A_1 := 1, \quad A_i := \prod_{k=1}^{i-1} \lambda^{(k)}, \quad i = 2, \dots, I, \quad (71)$$

$$A_{1,1} := 1, \quad A_{j,i} := \prod_{\substack{k=1 \\ k \neq j}}^i \frac{1}{\lambda^{(k)} - \lambda^{(j)}}, \quad i = 2, \dots, I. \quad (72)$$

The exact solution of the reaction equations can be used for the numerical solving of the general system (6) using the so-called *operator-splitting method*, see, e.g. [28].

6 General advection-reaction discretization scheme

The system of equations for the convective transport with decay reactions takes the form:

$$\partial_t \left(R^{(l)} \phi u^{(l)} \right) + \nabla \cdot \left(\mathbf{v} u^{(l)} \right) + \lambda^{(l)} R^{(l)} \phi u^{(l)} = \lambda^{(l-1)} R^{(l-1)} \phi u^{(l-1)}. \quad (73)$$

In general, we can use the exact scheme (70) for the decay part of (73) and the explicit discretization scheme (53) for the transport part. If the parameters $\theta^{(l)}$ for each component are not strongly different, i.e. $\theta^{(l)} \approx \theta$ for $l = 1, \dots, I$, then the operator-splitting approach (see [28]) only has a small temporal splitting error, and it can be successfully used for (73).

But in general, e.g. if the retardation factors are different, the convection and the reaction operator do not commute, and the standard operator-splitting method can have a large temporal splitting error.

Here we present a novel algorithm for the computations of (73).

Concretely, for each Ω_i and $j \in \text{out}(i)$, we have the following system of 1D convection-reaction equations for $l = 1, \dots, I$:

$$R_i^{(l)} \phi_i \partial_t u_i^{(l)} + v_{ij} \partial_x u_i^{(l)} + \lambda^{(l)} R_i^{(l)} \phi_i u_i^{(l)} = \lambda^{(l-1)} R_i^{(l-1)} \phi_i u_i^{(l-1)}. \quad (74)$$

The equation can be solved exactly for particular initial conditions, which is discussed in the next section 6.1. In the following, we consider the space variable $x \in (0, \infty)$, and the velocity $v_{ij} > 0$, given by (45).

We rewrite the concentration $c_i^{(l)} := R_i^{(l)} \phi_i u_i^{(l)}$ and the velocity $\tilde{v}_{ij} := \frac{v_{ij}}{R_i^{(l)} \phi_i}$ and obtain:

$$\partial_t c_i^{(l)} + \tilde{v}_{ij} \partial_x c_i^{(l)} + \lambda^{(l)} c_i^{(l)} = \lambda^{(l-1)} c_i^{(l-1)}. \quad (75)$$

Because of the time restriction, we first calculate the maximal time step for the cell j and the concentration i with respect to the total outflow fluxes,

$$\tau_{l,i} = \frac{V_i R^{(l)}}{\nu_i}, \quad \nu_i = v_{ij}, \quad j = \text{out}(i).$$

We get the restricted time step with the local time step of each of the cells and their underlying components

$$\tau^n \leq \min_{\substack{l=1, \dots, m \\ i=1, \dots, I}} \tau_{l,i}.$$

The velocity of the discrete equation is given as

$$v_{l,i} = \frac{1}{\tau_{l,i}}.$$

We calculate the analytical solution of the mass, see the next section 6.1, by using the equations (80) and (81). We obtain

$$\begin{aligned} m_{ij,rest}^{(l),n} &= m_1^{(l),n}(a, b, \tau^n, v_{1,i}, \dots, v_{l,i}, R^{(1)}, \dots, R^{(l)}, \lambda^{(1)}, \dots, \lambda^{(l)}), \\ m_{ij,out}^{(l),n} &= m_2^{(l),n}(a, b, \tau^n, v_{1,i}, \dots, v_{l,i}, R^{(1)}, \dots, R^{(l)}, \lambda^{(1)}, \dots, \lambda^{(l)}), \end{aligned}$$

where $a = V_i R^{(l)}(c_{ij}^{(l),n} - c_{ij'}^{(l),n})$, $b = V_i R^{(l)} c_{ij'}^{(l),n}$ and $m_i^{(l),n} = V_i R^{(l)} c_i^{(l),n}$ are the parameters and $j = out(i)$, $j' = in(i)$ are the indices of the flows. The linear impulse in the finite volume cell is constructed by $c_{ij'}^{(l),n}$ for the concentration on the inflow boundary and $c_{ij}^{(l),n}$ for the concentration on the outflow boundary of the cell i .

The discretization with the embedded analytical mass is calculated by

$$m_i^{(l),n+1} = m_{ij,rest}^{(l),n} + m_{j'i,out}^{(l),n},$$

where $m_{ij,rest}^{(l),n} = m_i^{(l),n} - m_{ij,out}^{(l),n}$ is the residual mass coming from the total mass and the outflow mass. The mass in the next time step is $m_i^{(l),n+1} = V_i c_i^{(l),n+1}$, and in the old time step it is the residual mass for the concentration l . The proof is done in [17]. In the next section we derive an analytical solution for the benchmark problem.

6.1 Exact mass solutions for 1D system of advection-reaction equations

For a simpler computation we transform the cell $\Omega_i = (0, L)$ to an unit cell $\Omega_i = (0, 1)$. We also have to arrange $c^{(l)} = R^{(l)} \phi u^{(l)}$ to obtain a simpler system of equations. For the one-dimensional mass solution the simpler equations are given as, see [17]:

$$m_1^{(l)} = \Lambda^{(l)} \sum_{i=1}^l \Lambda_i^{(l)} \exp(-\lambda_i t) \left(a \frac{(1-v_i t)^2}{2} + b(1-v_i t) - \sum_{\substack{j=1 \\ j \neq i}}^l \frac{1}{\lambda_{ij}} \right) - a(1-v_i t) \left(\sum_{\substack{j=1 \\ j \neq i}}^l \frac{1}{\lambda_{ij}} \right) + a \left(\sum_{\substack{j=1 \\ j \neq i}}^l \frac{1}{\lambda_{ij}} \left(\sum_{\substack{k \geq j \\ k \neq i}}^l \frac{1}{\lambda_{ik}} \right) \right), \quad (76)$$

where the factors λ_{ij} are defined as:

$$\lambda_{ji} = \lambda_{ij} := \frac{\lambda^{(i)} - \lambda^{(j)}}{v^{(i)} - v^{(j)}}, \quad (77)$$

and the factors $\Lambda^{(l)}$, $\Lambda_j^{(l)}$ and $\Lambda_{ij}^{(l)}$ are given as:

$$\Lambda^{(l)} = \prod_{i=1}^{l-1} \lambda_i, \quad \Lambda_i^{(l)} = \left(\prod_{\substack{j=1 \\ j \neq i}}^l \frac{1}{\lambda_j - \lambda_i} \right), \quad \Lambda_{ij}^{(l)} = \left(\prod_{\substack{k=1 \\ k \neq j \\ k \neq i}}^l \frac{\lambda_{ik}}{\lambda_{ik} - \lambda_{ij}} \right). \quad (78)$$

For the outflowing mass m_{i2} we compute the summation of the masses $m_{i_{ges}}$,

$$\begin{aligned} m_{ges}^{(l)} &= m_{impuls} c_{GDGL}^{(l)} \\ &= m_1^{(l)} + m_2^{(l)}. \end{aligned} \quad (79)$$

The total mass is given as

$$m_{ges}^{(l)} = \Lambda^{(l)} \left(\sum_{i=1}^l \Lambda_i^{(l)} \exp(-\lambda_i t) (a \frac{1}{2} + b) \right).$$

The outflowing mass is calculated as

$$m_2^{(l)} = m_{ges}^{(l)} - m_1^{(l)}.$$

For the discretization we get the following functions:

$$m_{ij,rest}^{(l),n}(\tau^n) = m_1^{(l)}(a, b, \tau^n, v_{1,i}, \dots, v_{l,i}, R^{(1)}, \dots, R^{(l)}, \lambda^{(1)}, \dots, \lambda^{(l)}), \quad (80)$$

$$m_{ij,out}^{(l),n}(\tau^n) = m_2^{(l)}(a, b, \tau^n, v_{1,i}, \dots, v_{l,i}, R^{(1)}, \dots, R^{(l)}, \lambda^{(1)}, \dots, \lambda^{(l)}), \quad (81)$$

where $a = R_i^{(l)} V_i (c_{ij}^{(l),n}(\tau^n) - c_{ij'}^{(l),n})$, $b = R_i^{(l)} V_i c_{ij'}^{(l),n}$ and $j \in out(i)$.

For the equations (80) and (81) we have used the one-dimensional outflow through the outflow boundary, given as

$$\nu_i = v_{ij}, \quad j = out(i), \quad (82)$$

where the CFL condition, that has to be fulfilled, is given as

$$\tau_{l,i} = \frac{V_i R_i^{(l)}}{\nu_i}.$$

Therefore the velocity for each cell i on the unit interval is given as

$$v_{l,i} = \frac{1}{\tau_{l,i}}.$$

Thus the resulting time step, used in (80) and (81), is given as $\tau^n \leq \min_{\substack{l=1,\dots,M \\ i=1,\dots,I}} \{\tau_{l,i}\}$.

For an illustration of the piecewise linear impulse applied for the mass solution in (76) we refer to the figure 3.

7 Diffusion-dispersion discretization scheme

We discretize the diffusion-dispersion equation with implicit time discretization and finite volume methods with constant test functions. We deal with the diffusion-dispersion equation given as

$$\partial_t R u - \nabla \cdot (D \nabla u) = 0, \quad (83)$$

where $u = u(x, t)$ with $x \in \Omega$ and $t \geq 0$. The diffusions-dispersions tensor is $D = D(x, \mathbf{v})$ given by the Scheidegger approach, cf. [31]. The velocity is given by \mathbf{v} and is piecewise constant in the cells. The retardation factor is $R > 0$.

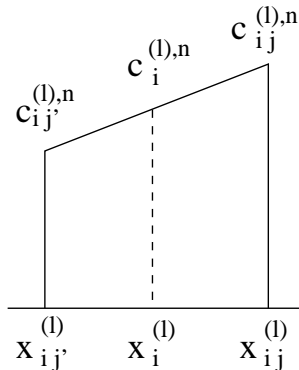


Fig. 3. Piecewise linear impulse given with the concentrations $c_{ij}^{(l),n}(\tau^n)$ and $c_i^{(l),n}$.

We have Neumann boundary values, given as $\mathbf{n} \cdot D \nabla u(x, t) = 0$, where $x \in \Gamma = \partial\Omega$, cf. [13]. The initial conditions are given as $c(x, 0) = c_0(x)$.

We integrate the equation (83) over space and time and get

$$\int_{\Omega_j} \int_{t^n}^{t^{n+1}} \partial_t R(c) dt dx = \int_{\Omega_j} \int_{t^n}^{t^{n+1}} \nabla \cdot (D \nabla c) dt dx. \quad (84)$$

We apply the backward Euler method and exactly integrate the left hand side of the equation (84). The right hand side is lumped for the diffusion-dispersion term, cf. [17], thus there holds:

$$\int_{\Omega_j} (R(c^{n+1}) - R(c^n)) dx = \tau^n \int_{\Omega_j} \nabla \cdot (D \nabla c^{n+1}) dx. \quad (85)$$

The equation (85) is discretized over the space with using the Greens formula. We obtain the following equation,

$$\int_{\Omega_j} (R(c^{n+1}) - R(c^n)) dx = \tau^n \int_{\Gamma_j} D \mathbf{n} \cdot \nabla c^{n+1} d\gamma, \quad (86)$$

where Γ_j is the boundary of the finite volume cell Ω_j . We use the approximation in space, cf. [17].

The integration of the equation (86) is done for finite boundaries. Using the middle-point rule yields:

$$V_j R(c_j^{n+1}) - V_j R(c_j^n) = \tau^n \sum_{e \in \Lambda_j} \sum_{k \in \Lambda_j^e} |I_{jk}^e| \mathbf{n}_{jk}^e \cdot D_{jk}^e \nabla c_{jk}^{e,n+1}, \quad (87)$$

where $|I_{jk}^e|$ is the length of the boundary element I_{jk}^e . The gradients are calculated with the piecewise finite element function ϕ_l and we get

$$\nabla c_{jk}^{e,n+1} = \sum_{l \in \Lambda^e} c_l^{n+1} \nabla \phi_l(\mathbf{x}_{jk}^e). \quad (88)$$

Because of the reconstruction of the gradient with the piecewise linear finite element functions, we obtain a second-order discretization method, cf. [15]. This leads to the following discretization form:

$$\begin{aligned} V_j R(c_j^{n+1}) - V_j R(c_j^n) &= \\ &= \tau^n \sum_{e \in A_j} \sum_{l \in A^e \setminus \{j\}} \left(\sum_{k \in A_j^e} |\Gamma_{jk}^e| \mathbf{n}_{jk}^e \cdot D_{jk}^e \nabla \phi_l(\mathbf{x}_{jk}^e) \right) (c_j^{n+1} - c_l^{n+1}), \end{aligned} \quad (89)$$

where $j = 1, \dots, m$.

In the next section we describe the operator-splitting methods, that are used to decouple the full equations.

8 Operator-splitting methods

The operator-splitting methods are used to decouple complicated partial differential equations into simpler equations and are often used in the geophysical and environmental physics. They are developed and applied in [33],[36] and [39].

The ideas based in this article are to solve simpler equations with higher-order discretization methods. For this aim we use the operator-splitting method and decouple the equation with respect to the different time scales into simpler equations. There are many possible ways to combine the methods to achieve an effective higher-order discretization method. One possibility is to discretize the convection equation with a characteristic method, the diffusion-dispersion equations with finite volume methods, and the reaction equations with exact methods. Another way would be to solve the convection-reaction equations with one mixed discretization method, and the diffusion-dispersion equation with finite volume methods.

In the following we consider the system of ordinary differential equations given as

$$\partial_t c(t) = A c(t) + B c(t), \quad (90)$$

where the initial conditions are $c^n = c(t^n)$. The operators A and B are assembled by the spatial discretizations, e.g. the convection part with characteristic methods and the diffusion part with finite volume methods.

The operator-splitting method is introduced as a method, which solves the two equation parts sequentially with respect to the initial conditions. We get two simpler equations

$$\begin{aligned} \frac{\partial c^*(t)}{\partial t} &= A c^*(t), \quad \text{with } c^*(t^n) = c^n, \\ \frac{\partial c^{**}(t)}{\partial t} &= B c^{**}(t), \quad \text{with } c^{**}(t^n) = c^*(t^{n+1}), \end{aligned} \quad (91)$$

where the time step is $\tau^n = t^{n+1} - t^n$. The solutions of the equations are $c^{n+1} = c^{**}(t^{n+1})$.

The local splitting error of the sequential splitting method is given as, cf. [17]:

$$\rho_n = \frac{1}{2}\tau^n[A, B]c(t^n) + O((\tau^n)^2), \quad (92)$$

where $[A, B] := AB - BA$ is the commutator of A and B . We get an error $O(\tau^n)$, if the operators A and B do not commute, otherwise the method is exact.

We improve our method by the so-called *Strang splitting method*, which is of second order, cf. [33].

The method is presented as

$$\begin{aligned} \frac{\partial c^*(t)}{\partial t} &= Ac^*(t), \text{ with } t^n \leq t \leq t^{n+1/2}, c^*(t^n) = c^n, \\ \frac{\partial c^{**}(t)}{\partial t} &= Bc^{**}(t), \text{ with } t^n \leq t \leq t^{n+1}, c^{**}(t^n) = c^*(t^{n+1/2}), \\ \frac{\partial c^{***}(t)}{\partial t} &= Ac^{***}(t), \text{ with } t^{n+1/2} \leq t \leq t^{n+1}, c^{***}(t^{n+1/2}) = c^{**}(t^{n+1}), \end{aligned} \quad (93)$$

where the results of the method are $c^{n+1} = c^{***}(t^{n+1})$.

The splitting error of this method is given as, cf. [24],

$$\rho_n = \frac{1}{24}(\tau^n)^2([B, [B, A]] - 2[A, [A, B]])c(t^n) + O((\tau^n)^4), \quad (94)$$

where we get the second order for non-commuting operators.

For our methods it is sufficient to have second-order decomposition methods. Further higher-order splitting methods are described in the literature [8],[22] and [25].

In the next section we present the results of our numerical experiments.

9 Numerical experiments

9.1 Benchmark model

First, we illustrate the method of the section 6.1 on a simple 1D example with four components, where the porosity is ϕ and the retardation factors have the values $R^{(1)} = 1$, $R^{(2)} = 2$, $R^{(3)} = 4$ and $R^{(4)} = 8$. The numerical solution at the last computation time $t = 6$ is presented in figure 4 and it cannot be distinguished from the exact solution. The computations were realized with $\tau^n = \tau_{\text{CFL}}^n/2$, i.e. with the Courant number 0.5, the domain Ω is given as the interval $(0, 8) \subset \mathbb{R}^+$.

In the table 1, we compare the absolute error E_1 for the standard operator-splitting approach (the second column) and the equivalently defined error E_2 for the new algorithm (the fourth column). The results are presented for several uniformly refined grids and the numerical convergence rates are presented for the operator-splitting algorithm (the third column) and the new algorithm (the fifth

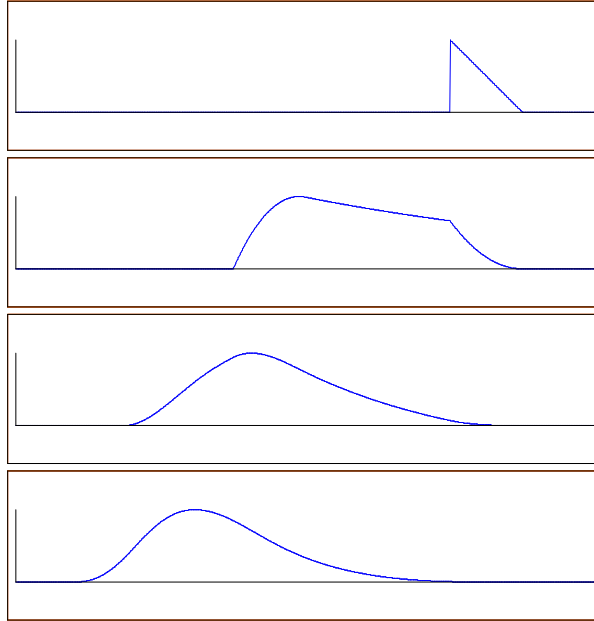


Fig. 4. Four components of the numerical solution for $t = 6$ with the retardation factors $R^{(1)} = 1$ (top), $R^{(2)} = 2$, $R^{(3)} = 4$ and $R^{(4)} = 8$ (bottom). The velocity is $v \equiv 1$ and the domain is $(0, 8) \subset R$.

column). As expected, for the operator-splitting method, the convergence rate is approximately 1, i.e. the absolute error is halved for one grid refinement, and the convergence rate for the new algorithm is approximately 2, i.e. the absolute error is four times smaller after one grid refinement.

h	$E_1 \cdot 10^{-4}$	α_1	$E_2 \cdot 10^{-4}$	α_2
1/16	413.2		23.76	
1/32	201.3	1.04	5.573	2.09
1/64	99.25	1.02	1.374	2.02
1/128	49.25	1.01	0.344	1.99

Table 1. The absolute error E_1 (operator-splitting method) and E_2 (the new algorithm) for the fourth component of the numerical solution. The third and fifth column contain the corresponding convergence rates.

In the next subsection we present complex scenarios in a waste disposal done in a salt dome.

9.2 Two-dimensional model of a waste disposal

We calculate some scenarios of waste cases, which help us to get new conclusions about the waste disposals in salt domes.

We have a model based on an overlying rock over a salt dome. We suppose an waste case, so that a permanent source of radioactive contaminant groundwater flows from the bottom of the overlying rock, where the waste disposal is suited. We suppose that the contaminants are flown with the groundwater, which is flown through the overlying rock. Based on our model we calculate the transport and the reaction of this contaminants coupled with decay chains. The simulation time is $10000[a]$ and we calculate the concentration, that is flown up to the top of the overlying rock. With this dates we can conclude, if the waste disposal is save enough. The two-dimensional test case is presented with the dates of our project partner GRS in Braunschweig (Germany), cf. [10] and [11].

We have a model domain with the size of $6000[m] \times 150[m]$ with four different layers with different permeabilities, see [10]. The domain is spooled with groundwater from the right boundary to the left boundary. The groundwater is flowing faster through the permeable layer than through the impermeable layers. Therefore the groundwater flows from the right boundary to the half middle of the domain. It is flowing through the permeable layer down to the bottom of the domain and spooled up in the left domain to the top. The groundwater flows in the left top part to the outflow at the left boundary. The flow field with the velocity is calculated with the program package **d³f** and presented in figure 5.

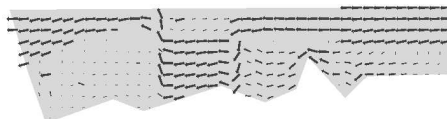
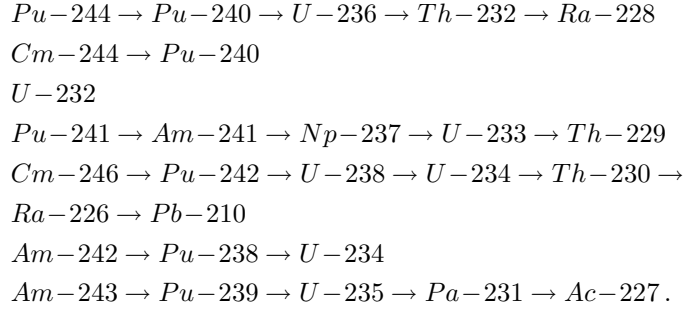


Fig. 5. Flow field for a two-dimensional calculation.

In the middle of the bottom of the domain, the contaminants are flown in as a permanent source. With the stationary velocity field, the contaminants are computed with the software package R^3T . The flow field transports the radioactive contaminants up to the top of the domain. The decay chain is presented

with 26 components as follows,



We present the important concentration in this decay chain. In the figure 6 the contaminant uranium isotope U-236 is presented after 100[a]. This isotope is less retarded and has a very long half-life period. Therefore the contaminant is flown furthest and decays less. This effect is presented in the figure 6. The diffusion process has spread out the contaminant in the whole left part of the domain. Also the impermeable layer is contaminated. After the time period of 10000[a], the contaminant is flown up to the top of the domain.

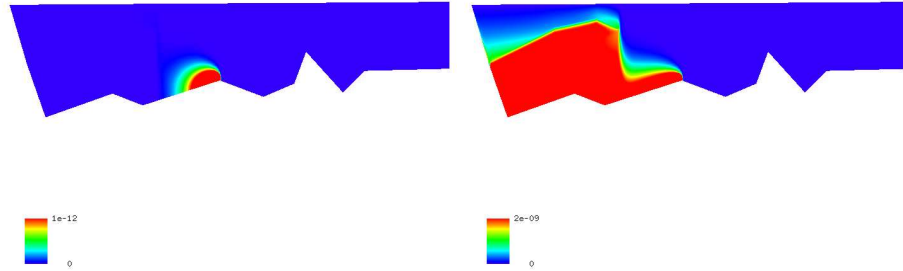


Fig. 6. Concentration of U-236 at the time point $t = 100[a]$ and $t = 10000[a]$.

The calculations are done on uniform grids. The convergence of this grids are confirmed with adaptive grid calculations. The calculation confirmed the results of finer and smaller time steps, cf. table 2. The beginning of the calculations is done with explicit methods until the character of the equation is more diffusive. Then we change to the implicit methods and can use larger time steps. With this procedure we can fulfill the forced maximum calculation time of one day.

Finally we conclude our paper with the next section.

Processors	Refinement	Number of elements	Number of time steps	Time for one time step	Total time
30	uniform	75000	3800	5 sec.	5.5 h.
64	adaptive	350000	3800	14 sec.	14.5 h.

Table 2. Computing the two-dimensional case.

10 Conclusions and discussions

We present discretization methods to solve a complex system of advection-diffusion-reaction equations. Based on the finite volume methods we present improved discretization methods for the convection-, diffusion-dispersion and convection-reaction equations. With a new embedding method for the analytical solutions we improve the discretization methods for the convection-reaction equations and we can skip the error in the temporal discretization. Second-order operator-splitting methods allow us to decouple the full equation system into simpler equations and to discretize each of them with higher-order finite volume methods. We verify the theoretical results with benchmark applications. Realistical test examples and the complex waste scenarios are presented. We can confirm, that a complex model could be simulated with the help of different splitting and discretization methods.

In the future we focus on the development of improved discretization methods and the idea of embedding local analytical solutions with the decoupling into simpler physical processes.

References

1. M. Abramowitz, I.A. Stegun. *Handbook of Mathematical Functions*, Dover Publication New York, 1970;
2. P. Bastian, K. Birken, K. Eckstein, K. Johannsen, S. Lang, N. Neuss, and H. Rentz-Reichert. *UG - a flexible software toolbox for solving partial differential equations*. Computing and Visualization in Science, 1(1):27–40, 1997.
3. H. Bateman. *The solution of a system of differential equations occurring in the theory of radioactive transformations*. Proc. Cambridge Philos. Soc., v. 15, pt V:423–427, 1910.
4. J. Bear. *Dynamics of fluids in porous media*. American Elsevier, New York, 1972.
5. J. Bear and Y. Bachmat. *Introduction to Modeling of Transport Phenomena in Porous Media*. Kluwer Academic Publishers, Dordrecht, Boston, London, 1991.
6. B. Davis. *Integral Transform and Their Applications*. Applied Mathematical Sciences, 25, Springer Verlag, New York, Heidelberg, Berlin, 1978 .
7. G.R.. Eykolt. *Analytical solution for networks of irreversible first-order reactions*. Wat.Res., 33(3):814–826, 1999.
8. I. Farago, J. Geiser. *Iterative Operator-Splitting Methods for Linear Problems*. IJCS, International Journal of Computational Sciences, Vol. 1, Nos. 1/2/3, pp. 64-74, October 2005.

9. E. Fein, T. Kühle, and U. Noseck. Entwicklung eines Programms zur dreidimensionalen Modellierung des Schadstofftransportes. *Fachliches Feinkonzept*, Braunschweig, 2001.
10. E. Fein. *Test-example for a waste-disposal and parameters for a decay-chain*. Private communications, Braunschweig, 2000.
11. E. Fein. *Physical Model and Mathematical Description*. Private communications, Braunschweig, 2001.
12. P. Frolkovič and J. Geiser. *Numerical Simulation of Radionuclides Transport in Double Porosity Media with Sorption*. Proceedings of Algorithmy 2000, Conference of Scientific Computing, 28-36, 2000.
13. P. Frolkovič. *Flux-based method of characteristics for contaminant transport in flowing groundwater*. Computing and Visualization in Science, 5(2):73-83, 2002.
14. P. Frolkovič and J. Geiser. *Discretization methods with discrete minimum and maximum property for convection dominated transport in porous media*. Proceeding of NMA 2002, Bulgaria, 2002.
15. P. Frolkovič and H. De Schepper. *Numerical modeling of convection dominated transport coupled with density driven flow in porous media*. Advances in Water Resources, 24:63-72, 2001.
16. J. Geiser. *Numerical Simulation of a Model for Transport and Reaction of Radionuclides*. Proceedings of the Large Scale Scientific Computations of Engineering and Environmental Problems, Sozopol, Bulgaria, 2001.
17. J. Geiser. *Gekoppelte Diskretisierungsverfahren für Systeme von Konvektions-Dispersions-Diffusions-Reaktionsgleichungen*. Doktor-Arbeit, Universität Heidelberg, 2004.
18. J. Geiser. *R³T : Radioactive-Retardation-Reaction-Transport-Program for the Simulation of radioactive waste disposals*. Proceedings: Computing, Communications and Control Technologies: CCCT 2004, The University of Texas at Austin and The International Institute of Informatics and Systemics (IIIS), 2004.
19. M.Th. Genuchten. *Convective-Dispersive Transport of Solutes involved in sequential first-order decay reactions*. Computer and Geosciences, 11(2):129-147, 1985.
20. GRAPE. *GRAphics Programming Environment for mathematical problems, Version 5.4*. Institut für Angewandte Mathematik, Universität Bonn und Institut für Angewandte Mathematik, Universität Freiburg, 2001.
21. W. Hackbusch. *Multi-Grid Methods and Applications*. Springer-Verlag, Berlin, Heidelberg, 1985.
22. E. Hairer, C. Lubich and G. Wanner. *Geometric Numerical Integration: Structure-Preserving Algorithms for Ordinary Differential Equations*. SCM, Springer-Verlag Berlin-Heidelberg-New York, No. 31, 2002.
23. K. Higashi und Th. H. Pigford. *Analytical models for migration of radionuclides in geologic sorbing media*. Journal of Nuclear Science and Technology, 17(9):700-709, 1980.
24. W.H. Hundsdorfer. *Numerical Solution od Advection-Diffusion-Reaction Equations*. Technical Report NM-N9603, CWI, 1996.
25. W. Hundsdorfer and J.G. Verwer. *Numerical Solution of Time-dependent Advection-Diffusion-Reaction Equations*. Springer Series in Computational Mathematics, 33, Springer Verlag, 2003.
26. W.A. Jury, K. Roth. *Transfer Functions and Solute Movement through Soil*. Birkhäuser Verlag Basel, Boston, Berlin, 1990 .
27. R.J. LeVeque. *Numerical Methods for Conservation Laws*. Lectures in Mathematics, Birkhäuser Verlag Basel, Boston, Berlin, 1992.

28. R.J. LeVeque. *Finite Volume Methods for Hyperbolic Problems*. Cambridge Texts in Applied Mathematics, Cambridge University Press, 2002.
29. T. Barth and M. Oehlberger. *Finite volume methods: foundation and analysis*. In: E. Stein, R. de Borst, T.J.R. Hughes (Eds.). *Encyclopedia of Computational Mechanics*, John Wiley & Sons, Ltd, 2004.
30. P.J. Roache. *A flux-based modified method of characteristics*. *Int. J. Numer. Methods Fluids*, 12:1259-1275, 1992.
31. A.E. Scheidegger. *General theory of dispersion in porous media*. *Journal of Geophysical Research*, 66:32-73, 1961.
32. Th. Sonar. *On the design of an upwind scheme for compressible flow on general triangulation*. *Numerical Analysis*, 4:135-148, 1993.
33. G. Strang. *On the construction and comparison of difference schemes*. *SIAM J. Numer. Anal.*, 5:506-517, 1968.
34. Y. Sun, J.N. Petersen and T.P. Clement. *Analytical solutions for multiple species reactive transport in multiple dimensions*. *Journal of Contaminant Hydrology*, 35:429-440, 1999.
35. V. Thomee. *Galerkin Finite Element Methods for Parabolic Problems*. Lecture Notes in Math., 1054, Springer Verlag, Berlin, Heidelberg, 1984.
36. J.,G. Verwer and B. Sportisse. *A note on operator splitting in a stiff linear case*. MAS-R9830, ISSN 1386-3703, 1998.
37. G. Wittum. *Multi-grid Methods : A introduction*. Bericht 1995-5, Institut für Computeranwendungen der Universität Stuttgart, Juni 1995.
38. H. Yserentant. *Old and New Convergence Proofs for Multigrid Methods*. *Acta Numerica*, 285-326, 1993.
39. Z. Zlatev. *Computer Treatment of Large Air Pollution Models*. Kluwer Academic Publishers, 1995.